ACADEMIA ROMÂNĂ
Revue Roumaine de Chimie
http://web.icf.ro/rrch/

Rev. Roum. Chim.,
2018, *63*(9), 829-835

Dedicated to Niculae I. Ionescu PhD
on the occasion of his 85th anniversary

THERMOSENSITIVE TRIBLOCK COPOLYMER TEMPLATED SYNTHESIS OF Pt-Cu SUPPORTED ON TiO_2: INVESTIGATION OF THEIR CATALYTIC ACTIVITY FOR CO OXIDATION REACTION

Daniela NEGOESCU,[a] Anca VASILE,[a] Veronica BRATAN,[a,*] Cristian HORNOIU,[a] Cornel MUNTEANU,[a] Mariana SCURTU,[a] Mircea TEODORESCU,[b] Irina ATKINSON,[a] Florica PAPA[a] and Ioan BALINT[a]

[a] "Ilie Murgulescu" Institute of Physical Chemistry, Roumanian Academy, 202 Splaiul Independenței, 060021 Bucharest, Roumania
[b] University Politehnica of Bucharest, Faculty of Applied Chemistry and Materials Science, 1-7 Gh. Polizu Street, 011061 Bucharest, Roumania

Received July 27, 2017

Pt-Cu/TiO_2 catalysts were prepared by two reductive deposition methods, using a thermosensitive triblock copolymer as template agent. The prepared catalysts were characterized using X-Ray Diffraction, SEM microscopy, EDX, UV-Vis Diffuse Reflectance Spectroscopy and CO pulse chemisorption measurements. The CO oxidation over Pt-Cu/TiO_2 materials was evaluated in order to investigate the impact of preparation methods on the catalytic performances.

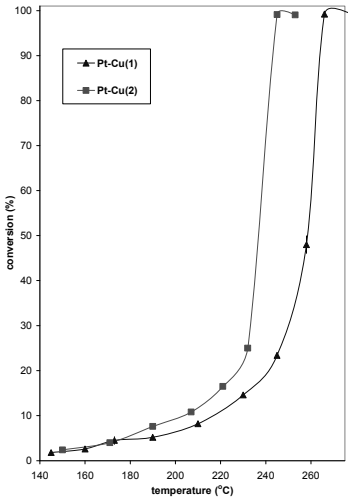

INTRODUCTION

Catalytic combustion is the main solution used to detect and remove the carbon monoxide, obtained from automotive emissions and industrial processes.[1,2] This method offers the advantage that CO can be removed from the effluents up to very low levels at relatively low temperatures. Typical combustion catalysts are noble metals, such as Pt, Pd, or Au dispersed on high surface area metal oxides like alumina, silica, or titania.[3-6]

Pt-based materials are considered to be the most prominent catalysts for VOCs oxidation.[7] The catalytic performance of these materials has been pointed out to be strongly dependent on the oxidation state and the size of the metal particles.[8-11]

* Corresponding author: vbratan@icf.ro

At lower temperatures CO strongly chemisorbs on Pt. This process stimulates a deactivation of catalyst.[12] Additionally, CO oxidation occurs at oxidized Pt nanoparticles providing another active sites and rising the catalytic activity.[13]

In recent years, it has been attempted to improve the catalytic performances by synthesizing intermetallic compounds. Bimetallic nanoparticles have shown higher catalytic activity compared with their monometallic equivalents. For example, $PtCu/Al_2O_3$ proved to be very active in preferential CO oxidation.[14,15] The CO conversion is found to be improved by Pt-Cu interactions.[16] The copper species is considered as a redox partner in the bimetallic supported catalyst: CO is adsorbed on the small metal crystals and oxidized with oxygen provided by CuO founded in close contact to metal nanoparticles.[17,18]

In this paper we report on the synthesis of Pt-Cu/TiO_2 catalysts using new type of thermosensitive block copolymer as structure directing agent. The samples were characterized using XRD, SEM, EDX and UV-Vis Spectroscopy. The dispersion and size of Pt nanoparticles was estimated from CO chemisorption measurements. Their catalytic properties were evaluated in CO oxidation reaction.

EXPERIMENTAL

Sample preparation. The 1 wt% Pt-Cu/TiO_2 catalysts were prepared by two reductive deposition methods presented as follows:

(1) First sample, denominated as Pt-Cu(1), was prepared by reduction of hexachloroplatinic acid $H_2PtCl_6 \cdot 6H_2O$ (10^{-4} M) with H_2 in aqueous media in presence of acetate dehydrate Cu $(CH_3\text{-}COO)_2 \cdot 2H_2O$ (99.7%), Merck, (10^{-4} M) and of a thermosensitive triblock copolymer (10^{-3} M), with Poly(ethylene glycol), PEG4,000 as the middle block and 3 mol% N-t-butylacrylamide (TBAM) in the initial monomer mixture, as previously described.[19] The molar ratio between capping polymer and metal cation was 10:1. Prior reduction, the aqueous solution containing the thermosensitive copolymer was bubbled with Ar gas for 20 minutes, to remove air, and then with H_2 gas for 10 minutes. The reaction vessel was sealed tightly and kept in thermostated water bath for 20 hours at 34°C. This temperature is above the lower critical phase transition temperatures (LCST) which was 38 °C for the thermosensitive polymers with 3 mol% N-t-butylacrylamide (TB).[19] After that, the support, TiO_2-P25 (Aerosil, Japan), was added in the reaction vessel, followed by filtration and drying.

(2) The second sample, denominated as Pt-Cu(2), was prepared by reduction of hexachloroplatinic acid $H_2PtCl_6 \cdot 6H_2O$ (10^{-4} M) with H_2 in aqueous media in the presence of the same thermosensitive triblock copolymer (10^{-3} M) presented before. The aqueous solution was bubbled with Ar gas for 20 minutes, and then with H_2 gas for 10 minutes. The reaction vessel was sealed tightly and kept in thermostated water bath for 20 hours at 34°C. After that, Cu^{2+} from the acetate dehydrate Cu $(CH_3\text{-}COO)_2 \cdot 2H_2O$ (10^{-4} M) was added and the obtained colloidal solution, containing metallic nanoparticles, was dispersed on the support,TiO_2-P25 (Aerosil, Japan), followed by filtration and drying.

Both samples were calcinated 1 hour at 400°C. The calculated metal loading was 1 wt%, with Pt-Cu as 1:1 molar ratio.

SEM and EDX analysis. The morphology of polycrystalline powders was studied by means of Scanning Electron Microscopy (SEM). The synthesized particles of Pt-Cu(1) and Pt-Cu(2) catalysts were characterized using high-resolution microscope, FEI Quanta 3D FEG, equipped with EDS Apollo X detector. The analyses were done in high vacuum mode, at an accelerating voltage of 20 kV with Everhart–Thornley secondary electron detector.

XRD measurements. The XRD patterns were collected by means of a Rigaku diffractometer type Ultima IV in parallel-beam geometry.

UV-Vis technique. The diffuse reflectance UV-Vis spectra were recorded using a spectrophotometer Perkin Elmer Lambda 35, equipped with integrating sphere. The measurements were carried out at room temperature in the range 1100-200 nm, using spectralon as a reference. The reflectance measurements were converted to absorption spectra using the Kubelka-Munk function, F(R).

CO pulse chemisorption. The exposed platinum surface area was estimated by CO pulse chemisorption performed at room temperature using a ChemBet-3000 Quantachrome Instrument equipped with a thermal conductivity detector (TCD). Prior to CO chemisorption measurements, the catalysts were reduced with H_2 at 400°C for 1 h.

Catalytic testing. Catalytic CO oxidation was performed in a flow reactor at atmospheric pressure. 60 mg of catalyst was placed between two glass wool plugs in quartz reactor. Prior to measurement of the catalytic activity, the catalysts were pretreated in helium atmosphere at 400°C for 1 hour. Activity measurements were performed as a function of temperature using a reactant mixture of 4.33 vol% CO and 13 vol% O_2 balance with He ($CO:O_2$ 1:3 molar ratio). The total flow rate was 30 ml/min, corresponding to a space velocity of 30,000 $mLh^{-1}g^{-1}$. The effluent gas was analyzed using an online gas chromatograph Perkin Elmer Clarus 500 equipped with a thermal conductivity detector. CO conversion was calculated as:

$$conversion(\%) = \frac{[CO]_{in} - [CO]_{out}}{[CO]_{in}} \cdot 100 \qquad (1)$$

where $[CO]_{out}$ represents the CO concentration after reaction (vol%) and $[CO]_{in}$ – its initial concentration (vol%).

RESULTS AND DISCUSSION

XRD measurements: The XRD pattern of the prepared samples and of the TiO_2 support are shown in Figure 1. The major crystal phases of the prepared samples was rutile and anatase. A characteristic peak of the (111) plane for metallic platinum (2θ =39.78°) appears (see inside Figure 1), revealing that Pt is essentially a face-centered cubic (fcc) structure.[20] No diffraction peaks for Cu species were observed, which may result from the low loaded content or fine dispersion of metal

species on the surface of TiO_2 particles. The diffraction angle of (111) plane from Pt obtained for Pt-Cu(1) and Pt-Cu (2) samples slightly shifts to higher values of 39.98° and 39.86°, respectively, caused probably by the introduction of some Cu into Pt.[21]

The crystalline phase composition could be calculated from experimental lattice value of the Pt-Cu nanoparticles using Vegard's law:[22,23]

$$a_{alloy} = x \cdot a_{Pt} + (1-x) \cdot a_{Cu} \qquad (2)$$

where a is the experimental lattice constant, x-the fraction of the Pt and a_{Pt}= 3.92 Å, a_{Cu}=3.61 Å.

The results for the lattice constant, determined from XRD peak positions were: 3.90 Å for Pt-Cu(1) and 3.91 Å for Pt-Cu(2). The calculated Pt metallic composition values, using equation (2), were: 93.5% for Pt-Cu(1) and 96.8% for Pt-Cu(2) respectively. These values indicated that platinum was not too much affected by the presence of copper, being only slightly alloyed with copper. For the Pt-Cu(2) sample, the percentage of alloy is lower, as is normal, considering that it was obtained by first precipitating the Pt, Cu being added after obtaining the Pt nanoparticles by reduction with H_2 in aqueous media.

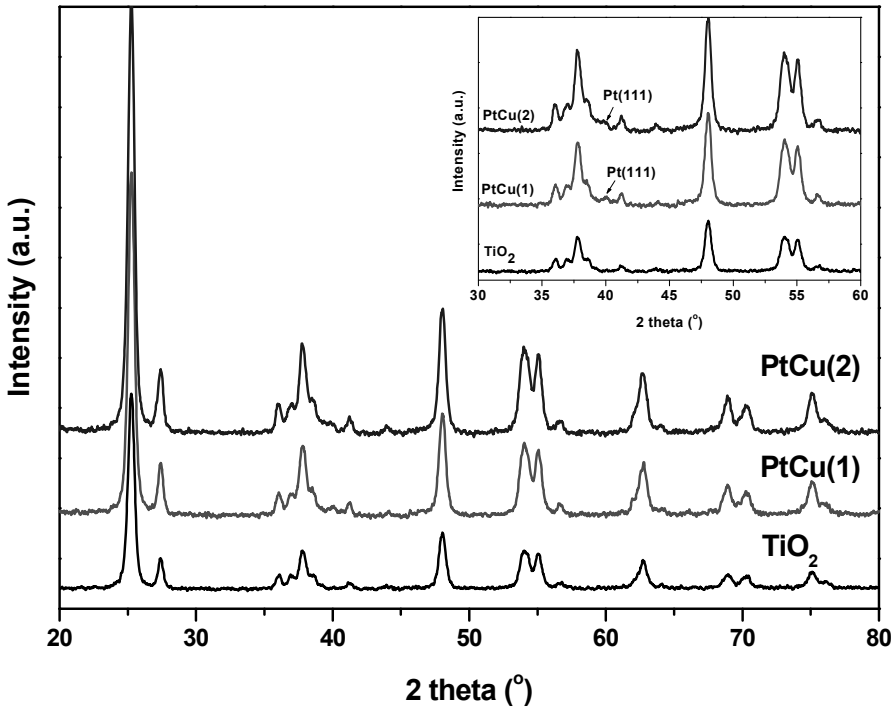

Fig. 1 – X-ray diffraction patterns of Pt-Cu(1) and Pt-Cu(2) catalysts.

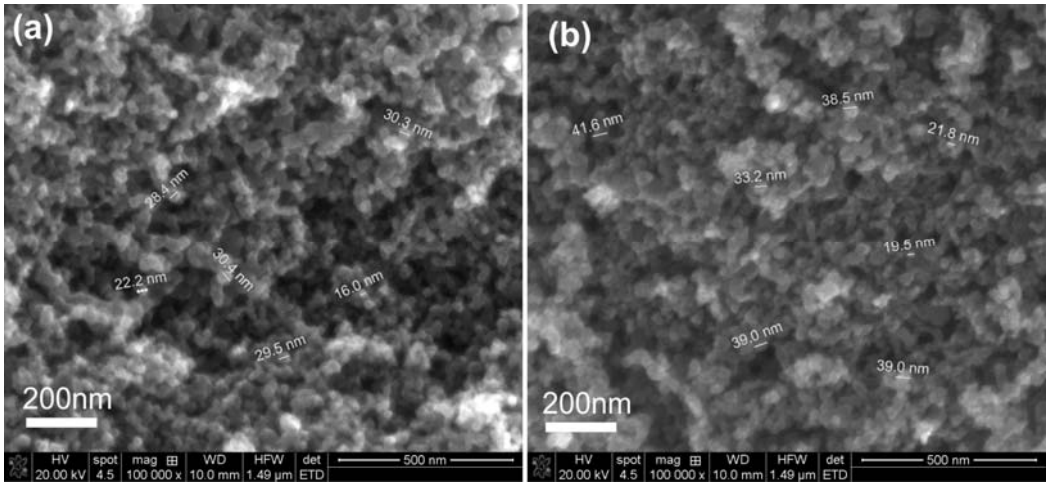

Fig. 2 – SEM images for (a) – Pt-Cu(1) and (b) – Pt-Cu(2) catalysts.

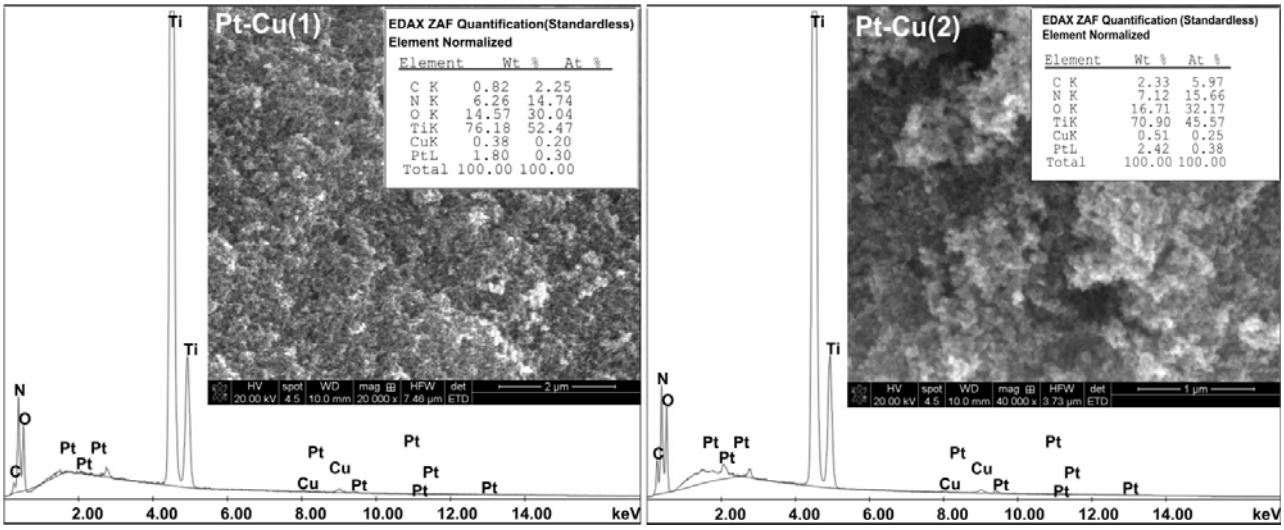

Fig. 3 – SEM-EDX Images for Pt-Cu(1) and Pt-Cu(2).

Table 1

EDX analysis of Pt and Cu contents on the surface of Pt-Cu/TiO_2 catalysts

Catalyst	Pt contents, (wt%)	Cu contents (wt%)
Pt-Cu(1)	1.80	0.38
Pt-Cu(2)	2.42	0.51

Table 2

The platinum dispersion (D) and particle size (d) obtained from CO pulse chemisorption; temperature of total conversion (T_{100}) and apparent activation energy (E_{app}) of the CO oxidation reaction

Catalyst	Dispersion, D (%)	Pt particle size, d (nm)	T_{100} (^oC)	Activation energy (KJ/mol)
Pt-Cu(1)	4.74	7.90	265	41.4
Pt-Cu(2)	3.16	11.90	245	47.3

SEM microscopy. The morphology of the Pt-Cu/TiO_2 catalysts was determined by SEM analysis and presented in Figure 2. The samples for the SEM analysis were prepared by direct deposition of powder on carbon tapes so agglomerates were observable. The SEM images showed the presence of small crystallites of titania support (less than 50 nm). Platinum and copper could not be observed, but were confirmed by EDX analysis.

The elemental composition of the samples was determined using the SEM-EDX analysis (Figure 3). The analysis confirmed the presence of oxygen, titanium, platinum and copper in the catalysts as expected.

In Table 1 there were listed the Pt and Cu contents as was obtained from EDX analysis. The higher values compared with those expected could be due to an enrichment of the metallic nanoparticles on the support surface after impregnation.

CO pulse chemisorption. The exposed platinum surface area was estimated by CO pulse chemisorption performed at room temperature. The measurements results, i.e the platinum dispersion (D) as well as the corresponding particle size ($d_{CO\ chem}$) were presented in Table 2.

Taking into account the preparation method, in case of the Pt-Cu(1) catalyst, both Pt and Cu NPs were pre-stabilized in the same colloidal suspension before their deposition on the TiO_2 surface according to the previously described procedure. This may suppress the Pt NPs growing on the surface, leading to smaller nanoparticles size. The presence of copper has a significant impact on the crystal growth and possible aggregation processes. In case of the Pt-Cu(2) catalyst, the first step in the preparation method was the Pt NPs formation in the colloidal suspension containing the polymer. It would seem that this stage has led to getting larger nanoparticles.

UV-Vis characterization. From diffuse reflectance spectra, presented in Figure 4, is clearly observed the influence of TiO_2 doping. An absorption peak at ~330 nm is present for all samples and is due to electronic transition from O2p to Ti3d.[24] For Pt-Cu samples the absorption edge is shifted to higher wavelength (~420 nm) and after this wavelength a broad absorption band is observed, due to the

presence of copper. Therefore, Cu(II) presents an absorption peak between 400-500 nm, appeared as a result of Cu(II) state attached to TiO_2 and an absorption band starting from 550 nm due to the d-d transition of Cu^{2+}.[24] So, from aborption spectra it could be concluded that copper is mainly in oxidized state. The facile oxidation of Cu catalyst in air was reported also elsewhere.[20,21]

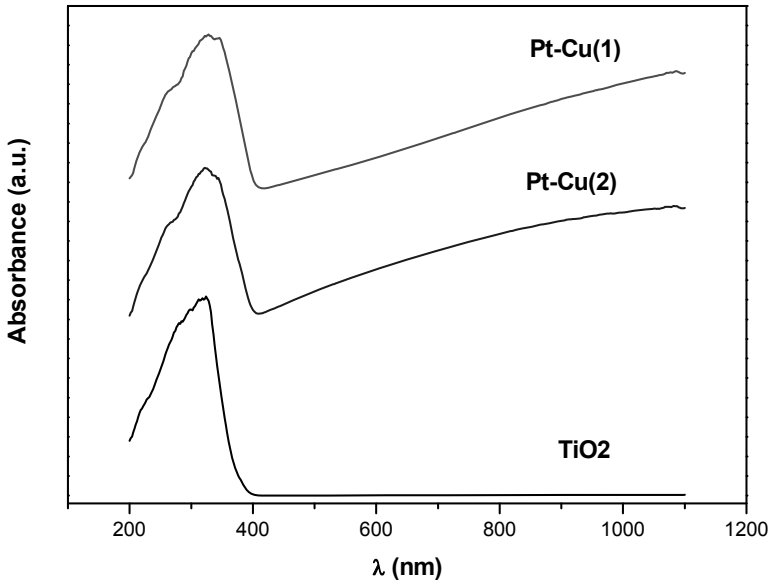

Fig. 4 – UV/vis spectra for calcined Pt-Cu(1), Pt-Cu(2) and TiO_2 (P25).

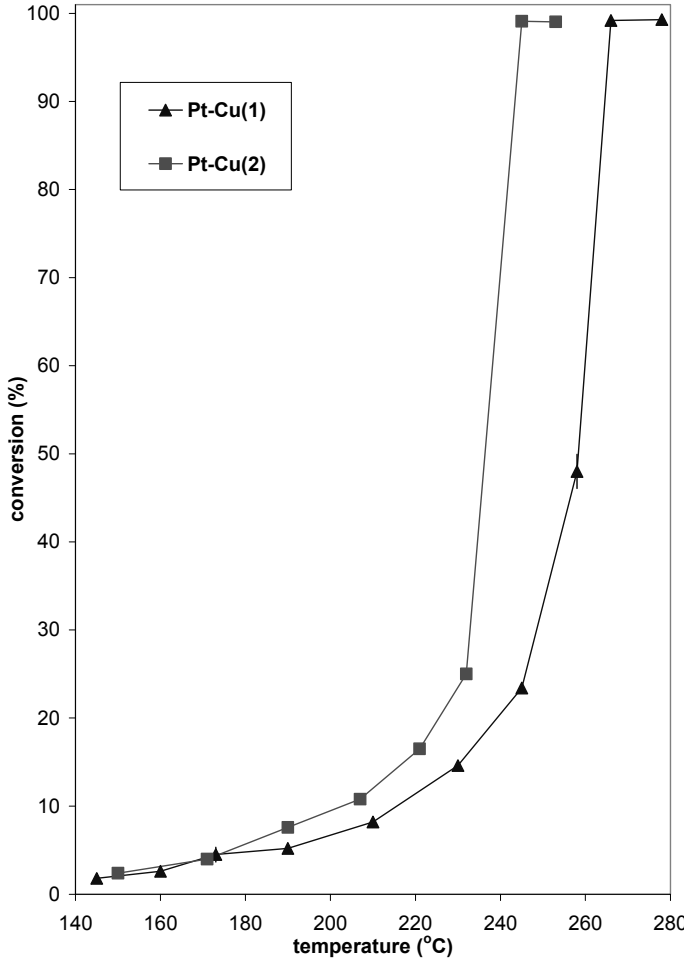

Fig. 5 – Conversion of CO over Pt-Cu/TiO_2 catalysts.

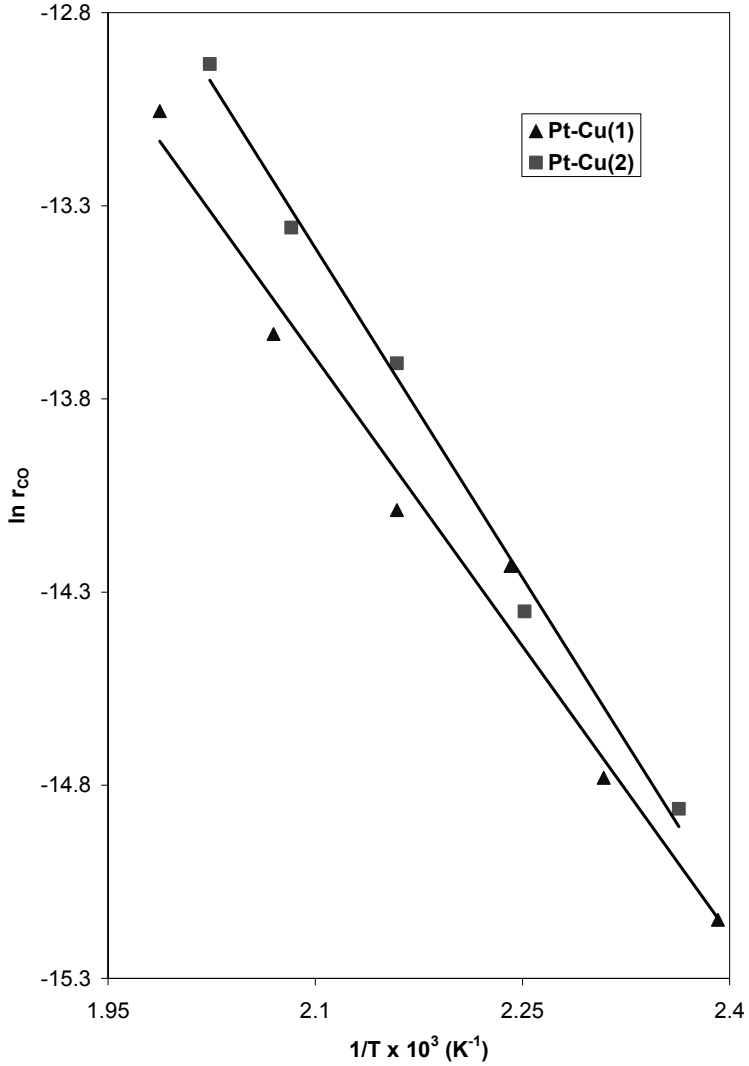

Fig. 6 – Logarithmic reaction rate of CO oxidation (measured in mol s^{-1} g_{cat}^{-1}) over Pt-Cu catalysts vs. of reciprocal temperature.

Platinum nanoparticles do not absorb in this domain and Pt^{4+} have an absorption peak centered at ~280 nm but it could not be observed due to overlapping with TiO_2 absorption.

Catalytic activity testing. The catalytic activity of the two samples was evaluated in CO oxidation. The experimental results, namely the variation of CO conversions with temperature over bimetallic Pt-Cu catalysts dispersed on a TiO_2 support, were shown in Figure 5.

As it could be seen, the samples have low conversions at temperatures up to 220°C. Additionally, in this temperature range the TiO_2 support has similar CO conversions (not shown here). For a comparison of catalytic activity, two parameters are used: temperature for 100% conversion of CO (T_{100}) and the apparent activation energy of reaction (E_{app}), obtained from the Arrhenius dependence of reaction rate (Figure 6). The values obtained are listed also in Table 2. The reaction rates were calculated based on a differential reactor from the data corresponding to %conversion of CO below 15%.

The apparent activation energy for both samples is lower than the value obtained for the CO oxidation on TiO_2 support (52.1 kJ/mol), indicating a better activity of the bimetallic supported samples. At the same time the measured E_{app} for Pt-Cu catalysts are slightly lower than previous measurements for CO oxidation over Pt/TiO_2 which is in the range of 50-60 kJ/mol.[25,26] The interaction of different platinum and copper species on TiO_2 support is proposed as one of the factors responsible for the kinetics difference of Pt-Cu(1) and Pt-Cu(2) samples prepared by methods with different stages. Usually the copper oxides are considered to improved the CO conversion at low temperatures due to their ability to provide oxygen for oxidation of CO, adsorbed on metallic Pt.[16-18]

At higher temperatures the conversion strongly increases for supported catalysts and the CO is

almost totally converted in CO_2 at 245°C for Pt-Cu(2) and 265°C for Pt-Cu(1). The support has only 40% conversion at 270°C.

It is generally accepted that CO oxidation on the supported noble metal catalysts proceeds via a Langmuir-Hinshelwood (L-H) reaction, between adsorbed CO and oxygen, metallic Pt being assigned as the active species.[5,27] The conversion is generally reduced at lower temperatures because CO is strongly adsorbed on Pt, resulting in unavailability of the oxygen activation.[12,28] At higher temperatures, in the studied case after 220°C, the strength of Pt-CO bonding decreases permitting the oxygen adsorption.

Although the weight percentages of Pt and Cu were exactly the same, the deposition of the thermosensitive triblock copolymer -stabilized colloidal solution, containing platinum nanoparticles, onto the TiO_2 support leads to more active catalysts at high temperatures, *i.e.* Pt-Cu(2), as compared with the other sample, i.e. Pt-Cu(1), where a pre-formed Pt–Cu colloidal solution was utilized for reduction with H_2 in aqueous media in presence of copper precursor. One factor that could be responsible for this different behavior at higher temperatures is the size of metallic Pt nanoparticles. The catalytic activity increases with the increase in particle size for Pt nanoparticles as it was observed previously.[29]

CONCLUSIONS

Pt-Cu/TiO_2 supported catalysts were developed and tested for CO oxidation. A thermosensitive triblock copolymer was used as the metals NPs structure directing agent. The prepared catalysts were characterized by XRD, SEM-EDX, UV-Vis techniques and CO pulse chemisorption measurements. The method employed to deposit Pt and Cu nanoparticles on TiO_2 affects the investigated catalytic process. The Pt-Cu(2) catalyst reaches the maximum conversion at a lower temperature than the Pt-Cu(1) catalyst.

Acknowledgements. Support of the EU (ERDF) and Roumanian Government that allowed for acquisition of the research infrastructure under POS-CCE O 2.2.1 project INFRANANOCHEM – Nr. 19/01.03.2009, is gratefully acknowledged.

REFERENCES

1. M. Haneda, M. Todo, Y. Nakamura and M. Hattori, *Catal. Today*, **2017**, *281*, 447.
2. M. Alifanti, M. Florea and V. I. Parvulescu, *Appl. Catal. B: Environ.*, **2010**, *95*, 327.
3. L. Liu, F. Zhou, L. Wang, X. Qi, F. Shi and Y. Deng, *J. Catal*., **2010**, *274*, 1.
4. B. Kalita and R. C. Deka, *J. Am. Chem. Soc.*, **2009**, *131*, 13252.
5. R. V. Gulyaev, A. I. Stadnichenko, E. M. Slavinskaya, A. S. Ivanova, S. V. Kosheev and A. I. Boronin, *Appl. Catal. A:Gen*, **2012,** *439-440,* 41.
6. M. Haruta, N. Yamad, T. Kobayashi and S. Iijima, *J. Catal*., **1989**, *115*, 301.
7. C. Chen, J. Zhu, F. Chen, X. Meng, X. Zheng, X. Gao and F.-S. Xiao, *Appl. Catal. B: Environ*, **2013**, *206*, 221.
8. N. Li, Q.-Y. Chen, L.-F. Luo, W.-X. Huang, M.-F. Luo, G.-S. Hu and J.-Q. Lu, *Appl. Catal. B: Environ*, **2013**, *142-143*, 523.
9. S. Cao, F. Tao, Y. Tang, Y. Li and J. Yu, *Chem. Soc. Rev.*, **2016**, *45*, 4747.
10. A. Naitabdi, R. Fagiewicz, A. Boucly, G. Olivieri, F. Bournel, H. Tissot, Y. Xu, R. Benbalagh, M.G. Silly, F. Sirotti, J.-J. Gallet and F. Rochet, *Top. Catal.*, **2016**, *59*, 550.
11. V. Bratan, C. Munteanu, C. Hornoiu, A. Vasile, F. Papa, R. State, S. Preda, D. Culita and N.I. Ionescu, *Appl. Cat. B: Env.*, **2017**, 207, 166.
12. F. Gao, Y. Wang, Y. Cai and D. W. Goodman, *J. Phys. Chem C*, **2009,** *113*, 174.
13. X. Yu, Y. Wang, A. Kim and Y. K. Kim, *Chem. Phys. Lett.*, **2017**, *685*, 282.
14. T. Komatsu, M. Takasaki, K. Ozawa, S. Furukawa and A. Muramatsu, *J. Phys. Chem C*, **2013**, *117*, 10483.
15. T. S. Mozer and F. B. Passos, *Int. J. Hydrogen Energy*, **2011**, *36*, 13369.
16. L.E. Gomez, B.M. Sollier, M.D. Mizrahi, J.M. Ramallo Lopez, E.E. Miro and A. V. Boix, *Int. J. Hydrogen Energy*, **2014**, *39,* 3719.
17. F. Wang, H. Zhang and D. He, *Env. Techn*., **2014**, *35*, 347.
18. K. I. Choi and M. A. Vannice, *J. Catal.*, **1991**, *127*, 489.
19. A. Vasile, M. Scurtu, C. Munteanu, M. Teodorescu, M. Anastasescu and I. Balint, *Process Saf. Environ. Prot.*, **2017**, *108*, 144.
20. W. H. Wang, X. L. Tian, K. Chen, and G. Y. Cao, *Colloids Surf. A: Physicochem. Eng. Asp.*, **2006**, *273*, 35.
21. H. Xiea, J. Y. Howe, V. Schwartz, J. R. Monnier, C. T. Williams and H. J. Ploehn, *J. Catal.*, **2008***, 259*, 111.
22. F. Papa, C. Negrila, A. Miyazaki and I. Balint, *J. Nanopart. Res.*, **2011**, *13*, 505.
23. F. Papa, A. Miyazaki, M. Scurtu, A. C. Ianculescu and I. Balint, *J. Nanopart. Res.*, **2014**, *16*, 2249.
24. B. Choudhury, M. Dey and A. Choudhury, *Intern. Nano Lett.*, **2013**, *3*, 25.
25. L. DeRita, S. Dai, K. Lopez-Zepeda, N. Pham, G.W. Graham, X. Pan and P. Cristopher, *J. Am. Cgem. Soc.*, **2017**, *139*, 14150.
26. G. R. Bamwenda, S. Tsubota, T. Nakamura and M. Haruta, *Catal. Lett.*, **1997**, *44*, 83.
27. L-Y. Jin, J.-Q. Lu, X.-S. Liu, K. Qian and M.-F. Luo, *Catal. Lett*.,**2009**, *128*, 379.
28. C. T. Campbell, G. Ertl, H. Kuipers and J. Segner, *J. Chem. Phys.*, **1980**, *73*, 5862.
29. G.W. Qin, W. Pei, X. Ma, X. Xu, Y. Ren, W. Sun and L. Zuo, *J. Phys. Chem.C*, **2010**, *114*, 6909.